ChemComm

Accepted Manuscript

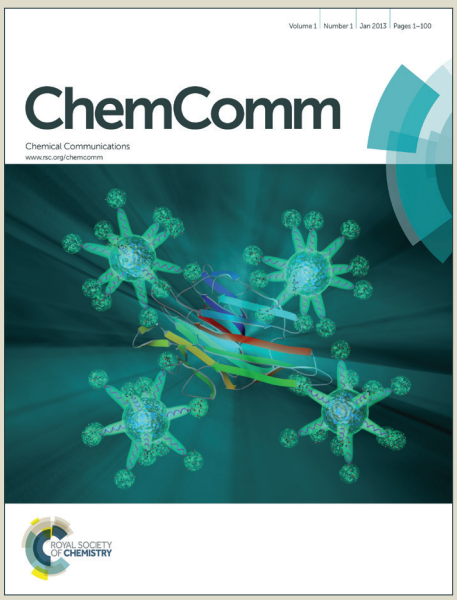

ROYAL SOCIETY OF CHEMISTRY

www.rsc.org/chemcomm

ChemComm

RSCPublishing

COMMUNICATION

A tumour mRNA-triggered nanocarrier for multimodal cancer cell imaging and therapy†

Cite this: DOI: 10.1039/x0xx00000x

Na Li, Huijun Yang, Wei Pan, Wei Diao and Bo Tang*

Received 00th January 2014,
Accepted 00th January 2014

DOI: 10.1039/x0xx00000x

www.rsc.org/chemcomm

We have established a tumour maker activated nanocarrier that can respond to the intracellular mRNA, allowing the multimodal cancer cell imaging and therapy.

Cancer is one of the world's most serious illnesses, accounting for several millions of deaths annually.[1] Cancer is usually treated with surgery, chemotherapy, radiotherapy, immunotherapy, and photodynamic therapy. For some cancers, combination therapy is the best approach because some therapies treat cancer that is confined locally and some therapeutic agents kill cancer cells that have spread to other parts of the body through the blood and lymph systems. Chemotherapy is the use of drugs in treating cancer that can kill these cells or stop them from multiplying, which is often used in conjunction with other cancer treatments. The therapeutic effect of chemotherapy is frequently restricted due to the limited solubility and instability of therapeutic agents, the nonspecific transport and poor permeability of drugs into tumour tissues.[2] Photodynamic therapy (PDT) as one of effective therapeutic methods combines photosensitizing agents that make cells sensitive to light and produce singlet oxygen under light irradiation.[3] PDT can directly kill cancer cells or act in other ways to shrink or destroy tumours. However, most of photosensitizers have a limited solubility in aqueous solution and therefore easily aggregate in the physiological environment, which could limit their applications in PDT. Several nanoparticle-based systems have been successfully introduced for imaging and therapeutic systems,[4] which may aid in evaluating therapeutic effects, improve the solubility and stability of drugs. Recently, a variety of nanocarriers have been explored for combined chemotherapy and PDT.[5] Compared to the single modal treatment, the therapeutic effect could be improved. Nevertheless, the nanocarriers distribute indiscriminately into all body cells and can be internalized into normal cells by an endocytosis process. To guide the development of therapy and enhance the therapeutic efficacy, it is highly desirable to develop an effective multimodal platform for simultaneous imaging and therapy.

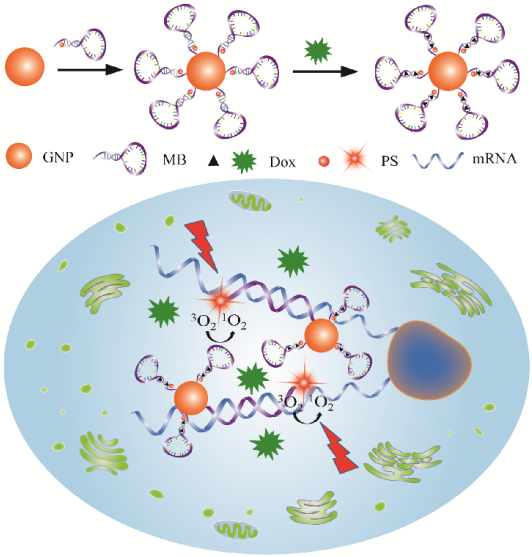

Scheme 1 Schematic illustration of the design and intracellular release of tumour mRNA-triggered nanocarrier.

In this study, we report a novel approach to construct tumour mRNA-triggered nanocarrier for chemotherapy and photodynamic therapy, enabling the activated release of chemotherapeutic agents and photosensitizers in cancer cells. The molecular beacon (MB) possesses a stem-loop structure and can be employed as the drug carrier for activated release.[6] The loop portion of the MB was designed with a complementary sequence to target nucleic acid and can recognize specifically target mRNA. The stem region of MB was formed by complementary arm sequences. Doxorubicin (Dox) as a chemotherapeutic agent can intercalate into the double-stranded

College of Chemistry, Chemical Engineering and Materials Science, Synergetic Innovation Center of Chemical Imaging Functionalized Probes, Key Laboratory of Molecular and Nano Probes, Ministry of Education, Shandong Normal University, Jinan 250014, P.R. China. E-mail: tangb@sdnu.edu.cn

† Electronic Supplementary Information (ESI) available: Experimental details and supporting figures. See DOI: 10.1039/b000000x/

GC or CG sequences of the stem region of MB, in which the fluorescence can be quenched and the cytotoxicity of Dox was decreased.[7] A photosensitizer moiety was linked to the end of one arm and the other arm attached to the surface of gold nanoparticles via gold-thiol bond. The GNPs have a strong surface plasmon absorption band in visible region and can effectively quench the fluorescence of the photosensitizer and Dox. When the nanocarrier encounters with the complementary targets, more stable duplexes were formed by the hybridization of MB and target sequences, causing the opening of MB and the release of Dox and PS molecules. The fluorescence and cytotoxicity of Dox were recovered. Meanwhile, the PS was activated for PDT and singlet oxygen was generated upon laser irradiation. The details of this approach are depicted in Scheme 1.

For the multimodal therapy strategy, chemotherapy and PDT are employed together to targeted kill cancer cells. First of all, a photosensitizer, chlorin e6 (Ce6), was modified to the MB to target intracellular TK1 mRNA. When it is conjugated with gold nanoparticles (GNPs), the Ce6 is non-phototoxic due to the quenching effect of GNPs. Then Dox intercalates into the double-stranded GC or CG sequences in the stem of the MB, which could quench the fluorescence and decrease cytotoxicity of Dox. It was calculated that two Dox molecules could intercalate into a single MB (see SI), which was consistent with the design of two double-stranded GC sequences for the MB. GNPs (13 nm) were utilized for the nanocarrier because GNPs are efficient quencher and can be densely modified with oligonucleotides.[8] It is noteworthy that a single GNP can carry multiple Ce6 and Dox into the cell, resulting in a high local concentration of photosensitizers and chemotherapy agents for more efficient destruction of the targeted cancer cells with fewer side effects. According to the previous protocol,[9] each GNP was calculated to carry about 50 MBs (see SI). The TEM images of GNPs and the nanocarriers were shown in Fig. S3. The border of the GNPs was clear while that of the nanocarrier was obscured, which indicated the MB was successfully assembled on the surface of GNPs. The UV-vis absorption spectra further confirmed the result, because the maximum absorption of the GNPs was red shifted from 519 to 523 nm when the nanocarrier formed (Fig. S4).

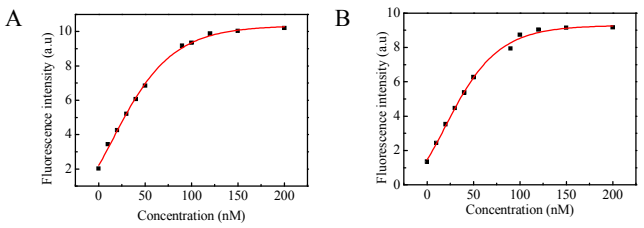

Fig. 1 Fluorescence curves of the nanocarrier (1 nM) in the presence of various concentrations of DNA target (0, 10, 20, 30, 40, 50, 100, 150, and 200 nM). A: Dox, B: Ce6.

To confirm that the fluorescence of Dox and Ce6 could be simultaneously triggered by DNA target, binding studies were performed with perfectly matched DNA target. As shown in Fig. 1, the fluorescence intensity of Ce6 and Dox was both increased along with the increase of DNA target concentrations from 0 to 200 nM. Moreover, the fluorescence intensity is relative to the concentration of DNA target, thus indicating that the hybridization of nanocarrier and target led to fluorescence recovery. Kinetic study indicated that the nanocarrier responded rapidly to the perfectly matched DNA target within about 5 minutes (Fig. S5). Fig. S6 showed that the nanocarrier was remarkably specific and sensitive to perfectly matched DNA target. Ce6 generated about 8-fold fluorescence increase and Dox produced about 5-fold fluorescence increase upon hybridization with the perfectly matched DNA target. By comparison, the signals did not obviously change in the presence of single-base-mismatched DNA target and other mismatched DNA targets and were of comparable magnitude to background.

The stability of the nanocarrier was investigated by monitoring the leakage of Dox. Fig. S7 showed that no more than 4% Dox was released after 30 days, which suggested the nanocarrier could provide effective retention of the drug molecules. After the nanocarrier was incubated with perfectly matched DNA target for 60 minutes, about 70% Dox molecules were released, suggesting that the nanocarrier could release the drug on demand. Nuclease stability is a key property of the DNA based nanocarrier for imaging and therapeutic applications in living cells. As shown in Fig. S8, the fluorescence intensity of Ce6 and Dox was not obviously changed before and after the treatment with enzyme deoxyribonuclease I (DNase I). While the fluorescence intensity of two agents was increased greatly after hybridization with the DNA target (Fig. S8, inset). The results further revealed that the release of Dox and Ce6 was indeed due to the hybridization of the nanocarrier with target instead of nuclease degradation and it suggested that the nanocarrier possessed high resistance to nuclease.

We next investigated the specificity of the nanocarrier for generating $^1O_2$ activated by DNA target. Disodium of 9,10-anthracenecliylbis-(methylene) dimalonic acid (ABMD) was employed to assess $^1O_2$ generation, because ABMD could react with $^1O_2$ to yield an endoperoxide, which causes a decrease in the intensity of ABMD absorbance.[10] The absorbance of ABMD is correlated negatively with the quantities of $^1O_2$.[11] The photo-oxidation of ABMD in the nanocarrier solution incubated with DNA target was monitored for 30 min upon irradiation with a diode laser at 655 nm. As shown in Fig. S9, the intensity of ABMD absorbance decreased continuously along with irradiation time from 0 to 30 min. However, in the absence of the DNA target, the ABMD absorbance did not show obvious change. The results indicated that the $^1O_2$ generation of the nanocarrier was specifically activated by the DNA target.

For the application of nanocarrier for targeted therapy in living cells, two couples of cells were chosen: human breast cancer cell line (MCF-7) where TK1 mRNA was overexpressed and normal immortalized human mammary epithelial cell line (MCF-10A) where TK1 mRNA was not overexpressed; human hepatocellular liver carcinoma cell line (HepG2) where TK1 mRNA was overexpressed and human hepatocyte cell line (HL-7702) where TK1 mRNA was not overexpressed. When MCF-7 cells were incubated with the nanocarrier, strong red fluorescence signal of Ce6 and green fluorescence signal for Dox were observed under confocal laser scanning microscopy (CLSM). (Fig. 2) After MCF-10A being incubated under the same condition, very faint fluorescence signals were observed, indicating that the TK1 mRNA expression was much higher in MCF-7 than in MCF-10A. After HepG2 cells being incubated with the nanocarrier, strong red and green fluorescence signals were observed under CLSM, which was similar with the case in MCF-7 cells. When HL-7702 cells were incubated with the nanocarrier, the phenomenon was also same as the case in MCF-10A cells. RT-PCR results further verified that the relative levels of TK1 in cancer cells were much higher than in normal cells. (Fig. S10).

The ability of the nanocarrier for releasing drugs according to the relative mRNA levels in living cells was evaluated. The relative levels of TK1 mRNA expression in HepG2 cells were down-regulated with tamoxifen and up-regulated with β-estradiol.[12] The HepG2 cells were separated into three groups in parallel. One group was treated with tamoxifen to decrease the

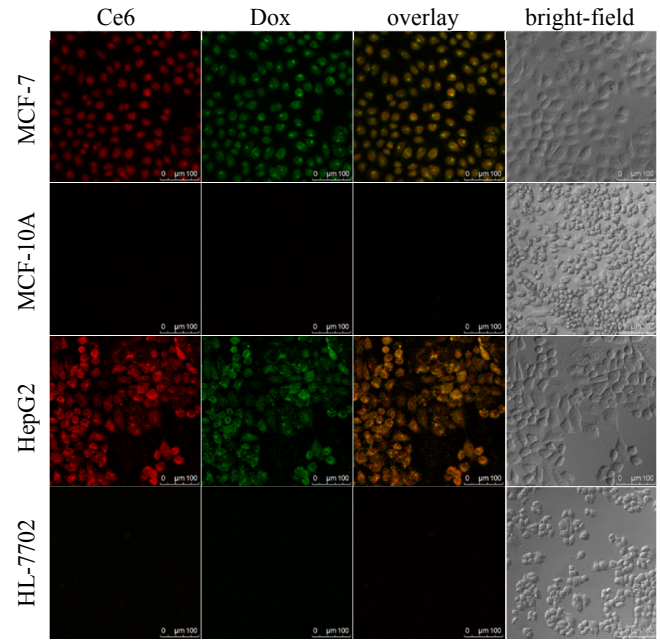

Fig. 2 Intracellular imaging of Dox and Ce6 under CLSM. MCF-7, MCF-10A, HepG2, and HL-7702 cells were incubated with the nanocarrier (1 nM) for 4 h at 37 °C. Ce6 was excited by 633 nm laser and Dox was excited by 488 nm laser, respectively. Scale bars are 100 μm.

TK1 mRNA expression and another one was treated with β-Estradiol to increase the TK1 mRNA expression. The untreated one was used as control. Next, the treated and untreated cells were incubated with the nanocarrier. Fig. S11 showed that the fluorescence intensities of Ce6 and Dox both decreased in the tamoxifen treated cells and increased in the β-estradiol treated cells. The bright-field images (Figure S9 d, e, f) suggested that the cells were viable throughout the imaging experiment. The results suggested that the release of drugs for the nanocarrier is dependent on the levels of mRNA in cancer cells.

MTT assay was performed to evaluate the multimodal therapeutic effect of the nanocarrier. The absorbance of MTT at 490 nm is dependent on the degree of activation of the cells. As shown in Fig. 3A, both the cancer cells and normal cells (without nanocarrier) showed slight decrease in cell viability after 20 min light irradiation, indicating the light irradiation showed almost no damage effect. When the cells were incubated with the nanocarrier, the PDT led to a decrease in breast cancer cell viability to about 59% and the chemotherapy led to a decrease in breast cancer cell viability to about 72%. Under the combination therapy of PDT and chemotherapy, the viability of breast cancer cells was dramatically dropped to below 32%. Interestingly, the cell viability of normal breast cells was always above 89% under single modal therapy or multimodal therapy. Similar results were obtained in liver cancer cells and normal liver cells (Fig. 3B). The results indicated the multimodal nanocarrier could efficiently increase the therapeutic effect for cancer cells, while it showed low toxicity for normal cells.

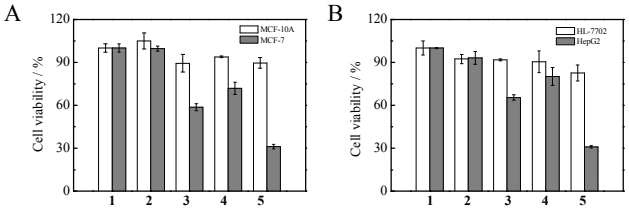

Fig. 3 MTT assay. A: MCF-7 and MCF-10A cells; B: HepG2 and HL-7702 cells. 1: control; 2: control with laser; 3: nanocarrier without Dox with laser; 4: nanocarrier with Dox without laser; 5: nanocarrier with Dox and laser.

In conclusion, we have demonstrated a tumour mRNA-triggered nanocarrier for multimodal imaging and therapy in living cells. The nanocarrier consists of gold nanoparticles functionalized with a dense shell of molecular beacons, in which the PS molecules and Dox were assembled and the fluorescence of them was quenched. The nanocarrier was silent in normal cells, but activated in response to the overexpressed mRNA in cancer cells. Moreover, the nanocarrier shows rapid response, high specificity and good biocompatibility. The nanocarrier could be triggered to release the Dox and PS molecules coupled with intracellular TK1 mRNA in cancer cells. Compared with single treatment, the nanocarrier could enormously enhance the therapeutic effect of in cancer cells when used for combination therapy. The current nanocarrier could effectively destroy cancer cells and protect the normal cells. Moreover, the nanocarrier could monitor the changes of the expression level of tumour mRNA and release Dox and PS controllably in cancer cells, which would be advantageous for cancer therapy. We envision that the current strategy could provide new insights for the design of multimodal imaging and therapy platform.

This work was supported by 973 Program (2013CB933800), National Natural Science Foundation of China (21227005, 21390411, 91313302, 21035003, 21375081, 21105059) and Program for Changjiang Scholars and Innovative Research Team in University.

Notes and references

1 World Health Organization. The Global Burden of Disease: 2004 Update. Geneva: World Health Organization, 2008; Latest world cancer statistics of International Agency for Research on Cancer, Available at: http://www.iarc.fr/en/media-centre/pr/2013/pdfs/pr223_E.pdf.
2 M. Ding, J. Li, X. He, N. Song, H. Tan, Y. Zhang, L. Zhou, Q. Gu, H. Deng, Q. Fu, *Adv. Mater.* 2012, **24**, 3639.
3 D. E. Dolmans, D. Fukumura, R. K. Jain, *Nat. Rev. Cancer* 2003, **3**, 380.
4 D. Peer, J. M. Karp, S. Hong, O. C. Farokhzad, R. Margalit, R. Langer, *Nat. Nanotechnol.* 2007, **2**, 751; J. Kim, Y. Piao, T. Hyeon, *Chem. Soc. Rev.* 2009, **38**, 372; R. A. Petros, J. M. DeSimone, *Nat. Rev. Drug Discov.* 2010, **9**, 615; W. Pan, H. Yang, T. Zhang, Y. Li, N. Li, B. Tang, *Anal. Chem.* 2013, **85**, 6930.
5 J. Hongrapipat, P. Kopečková, J. Liu, S. Prakongpan, J. Kopeček, *Mol. Pharmaceutics* 2008, **5**, 696; C.-L. Peng, P.-S. Lai, F.-H. Lin, S. Y.-H. Wu, M.-J. Shieh, *Biomaterials* 2009, **30**, 3614; T. Wang, L. Zhang, Z. Su, C. Wang, Y. Liao, Q. Fu, *ACS Appl. Mater. Interfaces* 2011, **3**, 2479.
6 B. Dubertret, M. Calame, A. J. Libchaber, *Nat. Biotechnol.* 2001, **19**, 365; S. Song, Z. Liang, J. Zhang, L. Wang, G. Li, C. Fan, *Angew. Chem. Int. Ed.*, 2009, **48**, 8670; Y. Gao, G. Qiao, L. Zhuo, N. Li, Y. Liu, B. Tang, *Chem. Commun.* 2011, **47**, 5316.
7 P. Fan, A. K. Suri, R. Fiala, D. Live, D. J. Patel, *J. Mol. Biol.* 1996, **258**, 480; G. Qiao, L. Zhuo, Y. Gao, L. Yu, N. Li, B. Tang, *Chem. Commun.* 2011, **47**, 7458.
8 C. A. Mirkin, R. L. Letsinger, R. C. Mucic, J. J. Storhoff, *Nature* 1996, **382**, 607; N. Li, C. Chang, W. Pan, B. Tang, *Angew. Chem. Int. Ed.* 2012, **51**, 7426.
9 L. M. Demers, C. A. Mirkin, R. C. Mucic, R. A. Reynolds, R. L. Letsinger, R. Elghanian, G. Viswanadham, *Anal. Chem.* 2000, **72**, 5535.
10 B. A. Lindig, M. A. J. Rodgers and A. P. Schaap, *J. Am. Chem. Soc.* 1980, **102**, 5590.
11 R. R. Zhang, C. L. Wu, L. L. Tong, B. Tang and Q. H. Xu, *Langmuir* 2009, **25**, 10153.

12 A. Kasid, N. E. Davidson, E. P. Gelmann, M. E. Lippman, *J. Bio. Chem.* 1986, **261**, 5562; J. A. Foekens, S. Romain, M. P. Look, P. M. Martin, J. G. M. Klijn, *Cancer Res.* 2001, **61**, 1421.

